Heliyon 9 (2023) e20280

Contents lists available at ScienceDirect

Heliyon

journal homepage: www.cell.com/heliyon

Fabrication of pH-dependent solid dispersion for oral colon-targeted delivery of notoginsenoside R1 and its protective effects on ulcerative colitis mice☆

Hongyun Tie [a,b,1], Yaru Wang [a,1], Yunxia Shang [a], Manlin Li [a,*], Xiaohui Wei [a,**], Zhengtao Wang [a]

[a] The MOE Key Laboratory for Standardization of Chinese Medicines and the SATCM Key Laboratory for New Resources and Quality Evaluation of Chinese Medicines, Institute of Chinese Materia Medica, Shanghai University of Traditional Chinese Medicine, Shanghai 201210, China
[b] Seventh People's Hospital of Shanghai University of Traditional Chinese Medicine, Shanghai 200137, China

ARTICLE INFO

Keywords:
Notoginsenoside R1
Solid dispersion
Colon-targeted drug delivery system
Ulcerative colitis

ABSTRACT

Notoginsenoside R1 (R1), which originated from the rhizomes and roots of Panax notoginseng, is classified as a Biopharmaceutical Classification System class III drug with good solubility but poor oral absorption. Although R1 can alleviate the inflammation of dextran sulfate sodium (DSS)-induced colitis in mice, the problem of acid degradation and low bioavailability limit its application. The purpose of this study was aimed to design one kind of pH-dependent solid dispersion for oral colon-targeted delivery of R1. Using Eudragit S100 (ES 100) and PEG 4000 as the pH-dependent carriers, R1 solid dispersion (R1-SD) was fabricated by solvent evaporation method. Scanning electron microscopy, differential scanning calorimetry, and powder X-ray diffraction analysis indicated that R1-SD was completely formed, the surface was smooth surface and the strip crystal structure of R1 disappeared. The *in vitro* release profile of R1-SD (R1-ES 100-PEG 4000, 1:7:1, weight ratio) exhibited that R1-SD was not released in media simulating the gastric condition (pH 1.2), but better release characteristics of the drug could be obtained in media simulating the intestinal condition (less than 30% in pH 6.8 phosphate-buffered saline and more than 90% in pH 7.6 condition). The *in vitro* colon absorption test showed that the absorption rate and cumulative release of R1-SD were higher than those of R1. R1-SD and R1 had apparent protective effect on colon shortening, inflammatory infiltrating tissue injury, weight loss, diarrhea, blood stool in mice with ulcerative colitis induced by DSS, and the protective effect of R1-SD was better than that of R1, which indicated R1-SD has good practical application prospects.

1. Introduction

Notoginsenoside R1 (R1, Fig. 1), one kind of protopanaxatriol saponins which isolated from *Panax notoginseng* (Burk.) F. H. Chen, is proved to have a great many of pharmacologic activities, including neuroprotective [1], anti-inflammatory [2], cardioprotective [3],

☆ Xiaohui Wei reports financial support was provided by the Shanghai Municipal Education Commission.
* Corresponding author.
** Corresponding author. Institute of Chinese Materia Medica, Shanghai University of Traditional Chinese Medicine, Shanghai 201210, China.
E-mail addresses: manlinli_cn@163.com (M. Li), xhweixh@163.com (X. Wei).
[1] Contributed equally to this work.

https://doi.org/10.1016/j.heliyon.2023.e20280
Received 5 January 2023; Received in revised form 12 September 2023; Accepted 18 September 2023
Available online 19 September 2023

and anticancer effects [4]. Our previous studies have shown that R1 could mitigate the inflammatory reaction of dextran sulfate sodium (DSS)-induced colitis in mice by reducing cytokines production, inhibiting the activity of myeloperoxidase, decreasing the expression of proinflammatory genes, and restraining the phosphorylation of IkBα, IkB kinase, and p65 in the colon [5]. However, R1 is classified as a Biopharmaceutical Classification System III drug [6,7] and liable to degradation in the gastric acid environment [8] with poor oral bioavailability [9,10], which limits its clinical application.

Oral colon-targeted drug delivery system (OCTDDS) is one new type of targeted drug delivery systems that utilize drug delivery technology to maximize the delivery of oral drugs to the colon for release and achieve the local or systemic therapeutic effects [11–14]. OCTDDS can be used to treat a series of local diseases related to colon, for instance, Crohn's disease, hemorrhagic enteritis, irritable bowel syndrome, ulcerative colitis (UC), colorectal cancer, etc. It can also be used to treat asthma, angina pectoris, arthritis, and other diseases with time rhythm [15,16]. OCTDDS is mainly divided into several types, such as pH-dependent drug release system, time-dependent drug release system, intestinal pressure-dependent drug release system, multi-trigger drug release system, and enzyme response drug release system. Among them, pH-dependent drug release system is on account of the different pH of human gastrointestinal tract to achieve colon-targeted drug release.

For the sake of achieving the effect of colon pH-dependent drug release, Eudragit S100 (ES 100), the colon soluble material, is usually selected as the pH-sensitive material to achieve the purpose that let drug does not release in stomach, not or a bit release in small intestine [17–21]. Drug molecules, colloidal, microcrystalline, or amorphous state can be highly fragmented in ES 100 to form a solid dispersion (SD) system, which could improve the dissolution and bioavailability. The main characteristic of SD is the use of carriers with different properties to keep drugs in a highly dispersed state, achieving different requirements for drug use purposes. The use of strong hydrophilic carriers can increase the solubility and dissolution rate of insoluble drugs, thereby improving the bioavailability of drugs. The use of insoluble carriers can delay or control drug release. Alternatively, enteric soluble carriers can be used to control drug release in the small intestine. Secondly, the encapsulation effect of the carrier can delay the hydrolysis and oxidation of drugs, cover up the unpleasant odor and irritation of drugs, and solidify liquid drugs, etc. Maghsoodi et al. [22] used ES 100 as the carrier to fabricate enteric release SD of piroxicam (PX) by spherical crystallization technique. The *in vitro* dissolution results showed that the drug did not release in pH 1.2 phosphate-buffered saline (PBS) while an obvious increase in dissolution of PX dispersed in ES 100 was noted in pH 7.4 PBS. SD can not only improve the dissolution rate but also the dispersion uniformity of the drug by transforming the drug from the original crystalline state to the amorphous state, so as to enhance the permeability and make the drug be absorbed more easily [23–26]. SD is a promising new formulation technology and with the advancement of global medical technology, the SD market will further develop.

In this study, a pH-dependent colon-soluble SD was fabricated to improve the stability and intestinal absorption of R1. Then, the preparation was characterized by scanning electron microscopy (SEM), powder X-ray diffraction (PXRD), and differential scanning calorimetry (DSC). Besides, the dissolution and release properties, the absorption in small intestine and protective effect on UC mice of the preparation were also studied.

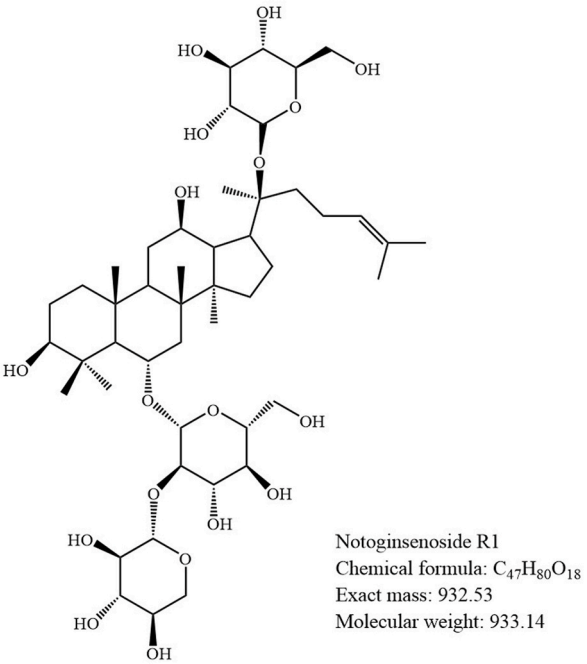

Fig. 1. The chemical structure of R1.

2. Materials and methods

2.1. Materials

R1 (the active ingredient, purity >98%) was purchased from Chengdu Purify Biotechnology Co., LTD. (Sichuan, China). ES 100 was provided by Shanghai Chine-way Pharmaceutical Accessories Co., LTD. (Shanghai, China). Polyethylene glycol (PEG 4000, PEG 6000) were purchased from Dalian Meilun Biological Technology Co., LTD. (Dalian, China), and hydrogenated soybean phosphatidylcholine (HSPC 100, purity >99%) was supplied by Lipoid GmbH (Ludwigshafen, Germany). DSS (molecular mass 36–50 kDa) was provided by MP Biomedicals (Solon, USA). Acetonitrile was chromatographic purity. The other reagents were all analytical pure grade.

2.2. Animals

SD rats (male, weight 300 ± 30 g) and eight-week-old C57BL/6 mice (female, weight 20 ± 2 g) were both purchased from the Shanghai Laboratory Animal Center (Shanghai, China) and raised in Animal Experiment Center of Shanghai University of traditional Chinese Medicine (Production license: ACSHU-2018-9180). This study protocol was conformed to the ethical guidelines authorized by the Animals Ethics Committee of Shanghai University of Traditional Chinese Medicine (animal ethics number: PZSHUTCM202023016). All animal studies were complied with the ARRIVE guidelines.

The animals were kept in plastic cages with two rats per cage and eight mice per cage, setting temperature at 25 ± 2 °C and 12 h light/dark cycle. The animals were free access to food and water.

2.3. R1 determination method

R1 concentration for *in vitro* release rate and intestinal absorption test were determined by Agilent 1260 Infinity Series HPLC system (Agilent Technologies, Santa Clara, CA, USA). By using a Platisil ODS column (4.6 × 250 mm, 5 μm) (Dikma Technologies, Beijing, China), R1 was detected with acetonitrile/water (20/80, v/v) as the mobile phase at 30 °C. The flow rate was set at 1.0 mL/min, the injection volume was 20 μL and the detection wavelength was 203 nm.

2.4. Preparation of R1 solid dispersions (R1-SD)

2.4.1. Selection of water-soluble excipients

R1-SD were prepared by solvent evaporation method. ES 100 is the basic carrier for the preparation of pH-dependent colon-targeted formulations. The addition of water-soluble excipients enables the rapid dissolution of drugs in the colon. Taking *in vitro* dissolution as the main investigation index, different water-soluble excipients (PEG 4000, PEG 6000, and HSPC 100) were added to investigate their effects on the cumulative release of R1 in ES 100 (3 copies were prepared in parallel).

2.4.2. Selection of the ratio of ES 100 to PEG 4000

The fixed reaction solvent was anhydrous ethanol, the concentration of R1 was 2 mg/mL, the stirring temperature was 45 °C, and the stirring speed was 800 rpm for 2 h. The ratio of ES 100 to PEG 4000 was screened using cumulative release *in vitro* as an index (3 copies were prepared in parallel).

2.4.3. Preparation of R1 solid dispersions (R1-SD)

R1, ES 100 and PEG 4000 (1:7:1, w/w/w) were put into ethanol to obtain a clear solution under the condition of stirring (800 rpm, 45 °C for 2 h). Then, the solvent was evaporated by a rotary evaporation equipment at 50 °C. The obtained solid material was dried in a vacuum drying furnace at 25 °C for 24 h, then ground with a mortar, and passed through a sieve (60-mesh).

2.4.4. Determination of R1 and R1-SD cumulative release in vitro

Samples were put into ordinary capsules respectively, each containing R1 50 mg, and tested at 37 °C and 100 rpm under the condition of pH 1.2 dilute hydrochloric acid buffer for 2 h, pH 6.8 PBS for 4 h, and pH 7.6 PBS for 8 h, respectively.

The same amount of 1 mL samples was withdrawn at regular intervals, filtered by a 0.45 μm syringe filter, and determined by an optimized HPLC method. The same amount of release medium was added to keep the volume constant. All results were from three separate experiments and reported as average values. The formula for calculating the cumulative dissolution is as follows:

Cumulative dissolution $= \frac{C_n V_2 + (C_{n-1} + \ldots + C_2 + C_1) V_1}{m} \times 100\%$.

C_n is the sample concentration at each time point, V_1 is the fixed volume taken for sampling at each time point, V_2 is the volume of dissolution medium, and m is the amount of R1 in the dissolution cup.

2.5. Characterization of R1-SD

2.5.1. Scanning electron microscopy (SEM)

Shape and surface morphology of R1, the physical mixture of R1, PEG 4000 and ES 100, the physical mixture of PEG 4000 and ES 100, and the R1-SD powder were all observed by SEM (8500-FE, Agilent, USA). The dried preparation samples were smeared on the

special sample table with conductive double-sided glue, and the sample table was placed in the ion sputtering instrument for surface gold plating (6 nm/min) in a vacuum of 60 s (6 Pa). The thickness of the film was 22 nm, and then observed by SEM.

2.5.2. Powder X-ray diffraction (PXRD)

R1, the physical mixture of R1, PEG 4000 and ES 100, the physical mixture of PEG 4000 and ES 100, and the R1-SD were measured by PXRD (Bruker D8 advance, Germany) under the condition of using Cu–K radiation with nickel filter under 40 kV, angle range 2θ between 3° and 40°, and counting time at 0.1 s per step.

2.5.3. Differential scanning calorimetry (DSC)

The thermal behaviors of R1, the physical mixture of R1, PEG 4000 and ES 100, the physical mixture of PEG 4000 and ES 100, and the R1-SD powder were studied by DSC (Q-2000, TA, USA). The samples were weighed in a standard open aluminum pan with the same empty pan as reference. The heating procedure was executed for each sample to run at a speed of 10 °C/min between 25 °C and 250 °C, while nitrogen was used as the purging gas. Indium was used to calibrate the temperature and heat flux *in vitro* dissolution and release of R1 and R1-SD capsules.

2.5.4. In vitro release of R1 and R1-SD

R1 and R1-SD were put into ordinary capsules respectively, each containing R1 50 mg. According to the third method of "Determination of Dissolution and Release" in the four general rules of the Chinese Pharmacopoeia (2020 edition), namely the small cup method, R1 capsules and R1-SD capsules were tested at 37 °C and 100 rpm in the following order: pH 1.2 dilute hydrochloric acid buffer for 2 h, pH 6.8 PBS for 4 h, and pH 7.6PBS for 8 h. Other operations were carried out according to the method under 2.4.4.

Following mathematical models were used to fit the drug release behavior of R1-SD in the condition of pH 7.6: (1) Zero-order release model: $Q = k\ t + b$; (2) First-order release model: $\ln (1\text{-}Q) = -k\ t + b$; (3) Higuchi model: $Q = k\ t^{1/2} + b$. Where Q is the drug release (%), t is the time of drug release.

2.6. In vitro intestinal absorption of R1 and R1-SD

According to the protocol, SD rats were divided into two groups randomly (group R1 and group R1-SD). Five rats in each group were fasted but free to water for 20 h before the experiment. After the rats being sacrificed with 3.5% chloral hydrate, a segment of ileum was carefully separated along the midline to remove mesentery and fat, taken for 10 cm, and washed with Krebs-Ringer buffer (118 mM NaCl, 4.7 mM KCl, 1.2 mM $MgSO_4$, 25 mM $NaHCO_3$, 1.2 mM KH_2PO_4, 2.5 mM $CaCl_2$, and 11 mM glucose, pH 6.8, 4 °C) [27–30].

Ligate the end of the ileum segment near bowel and secure the other end of the ileum to the orifice of the instrument (Fig. 2). 2 mL R1 and R1-SD aqueous solutions (both containing R1 6 mg/mL) were injected into the ileum with syringes, respectively. After ligating the orifice, the ileum segment was placed vertically in a McIntosh bath containing 15 mL Krebs-Ringer buffer.

The whole process of the experiment was maintained at 37 °C and in the water bath of 95% O_2/5% CO_2. After an equilibration of 5 min, 1 mL of samples were withdrawn according to the predetermined time interval (15, 30, 45, 60, 90, 120 min), and then filtered by a 0.45 μm syringe filter. The same amount of release medium was added to keep the volume constant. The concentration of R1 in each

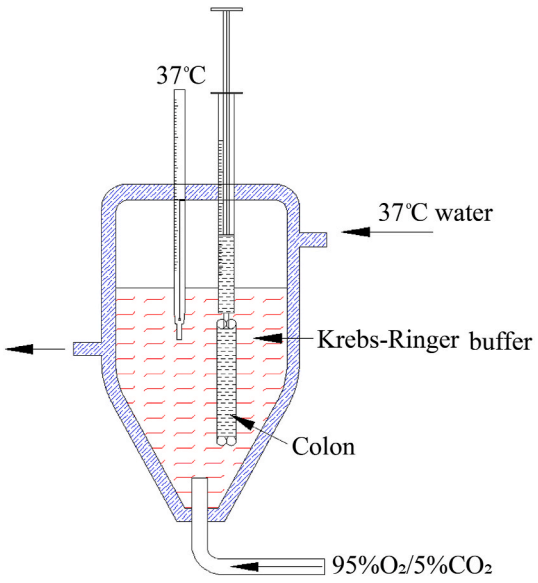

Fig. 2. The device of *in vitro* intestinal absorption test.

sample was determined via an optimized HPLC method and normalized by measuring the length of the sacs after incubation.

2.7. Protective effects on DSS colitis mice of R1 and R1-SD

DSS colitis model mice were induced according to references [31]. In this study, modeling and administration were conducted at the same time. In brief, the mice were administered with 4% (w/v) DSS aqueous solution successively for 9 days after a 2-day conventional feeding, whereas the mice in the vehicle group drank water instead (10 mice per group). Meanwhile, the mice in the R1 group and R1-SD group were administered with R1 (25 mg/kg) and R1-SD (equivalent to R1 25 mg/kg) in 0.5% CMC-Na for the 9 days, respectively. While the mice in the vehicle group and the model group were administered with 0.5% CMC-Na instead. The dosage of R1 was selected according to the results of the previous studies [5].

The severity of diarrhea was observed throughout the whole process of the experiment. After sacrificed under anesthesia, the mice colon length of was measured, and then the colons were separated and fixed in 10% formalin buffer. Histological examination (H&E) stain was performed after paraffin embedding. Histological scores were obtained through blind method by two pathologists according to the scoring roles for tissue damage (score 0–3) and inflammatory cell infiltration (score 0–3), as described previously [32–34]. Body weight and spleen weight were also recorded every day during the whole experiment.

2.8. Statistical analysis

Data are expressed as mean ± SD, and analyzed using GraphPad Prism 8. The data were tested by one-way ANOVA followed by post hoc analysis with Bonferroni's test, and $p < 0.05$ was considered to be statistically significant.

3. Results and discussion

3.1. R1 determination method

Quantitative analysis of R1 was performed via the HPLC 1260 system. Within the tested concentration range of 11.75–3000.00 μg/mL, the calibration curve of R1 was drawn by the corresponding concentrations (x, μg/mL) *versus* the peak areas (y) and expressed as $y = 4197.6\,x + 57.68$ ($r^2 = 0.999$). The recovery of R1 was between 98.79% and 103.22% (RSD < 2.14%). The repeatability and precision of inter- and intra-day were expressed by RSD value. Results showed that the peak areas repeatability was 2.68%, and the intra- and inter-day precision was below 2.70%. These results demonstrated that the optimized HPLC method was suitable for R1 quantitative determination.

3.2. Optimisation of R1-SD Procession

3.2.1. Confirmation of water-soluble excipients type

The results of the effect of different water-soluble excipients (PEG 4000, PEG 6000 and HSPC 100) on the cumulative percentage dissolution of R1 in the primary carrier ES 100 are shown in Fig. 3.

R1 was insoluble in all prescriptions except API at pH 1.2 (Fig. 3a). The cumulative dissolution in the condition of pH 6.8 for all prescriptions was lower than that of API, with 30% for PEG 4000, 40% for PEG 6000 and 42% for HSPC 100, respectively (Fig. 3b). At pH 7.6, the dissolution rate and final dissolution amount of PEG 6000 and HSPC 100 were similar, while the dissolution rate of PEG 4000 was significantly faster than that of PEG 6000 and HSPC 100, with a cumulative dissolution amount of 80% in 3 h (Fig. 3c).

According to the screening indexes of colonic preparations, PEG 4000 was selected as the water-soluble excipient based on the principles of pH 1.2 insolubility, pH 6.8 low solubility and pH 7.6 high solubility.

3.2.2. Determination of the ratio of ES 100 to PEG 4000

The results of the cumulative percent solubility of R1 in different formulations (R1:ES 100:PEG 4000 in the ratios of 1:3:1, 1:5:1, 1:7:1, 1:8:1, 1:9:1, and 1:9:2, respectively) are shown in Fig. 4.

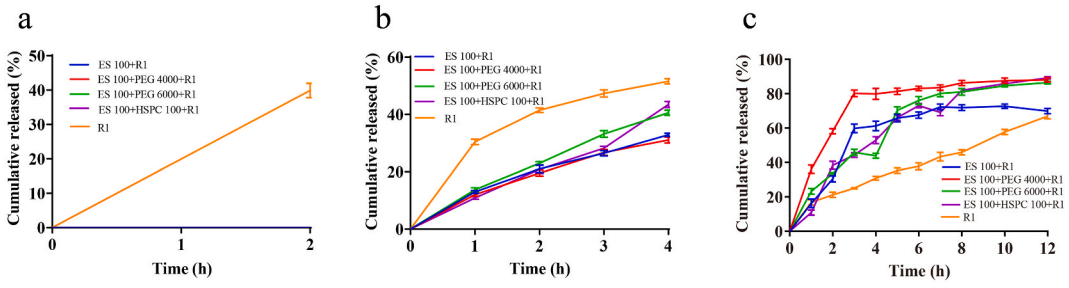

Fig. 3. *In vitro* cumulative releasing profiles of formulations with different water-soluble excipients. (a: pH 1.2. b pH 6.8. c pH 7.6).

R1 was not dissolved in any of the prescriptions except API at pH 1.2 (Fig. 4a). In the condition of pH 6.8, the cumulative amount of R1 dissolved in different prescriptions was relatively low and meet the requirements for colon preparations at the ratios of 1:7:1 (29.7%), 1:8:1 (30.9%), and 1:9:2 (31.6%)(Fig. 4b). At pH 7.6, the cumulative dissolution of R1 in different prescriptions was fastest and greatest at the three ratios of R1:ES 100:PEG 4000 of 1:5:1 (95.5%), 1:7:1 (97.8%) and 1:9:2 (95.8%) (Fig. 4c). According to the screening indexes of colonic preparations, R1:ES 100:PEG 4000 ratio 1:7:1 was selected as the prescription for R1-SD.

3.3. Characterization of the optimized R1-SD

3.3.1. SEM analysis

SEM, which reveals the surface morphology and internal structure of nanoscale particles, is usually used to characterize solid dispersions. Drugs form solid dispersions generally in an amorphous state [35].

SEM photographs are shown in Fig. 5. Free R1 appeared as prismatic crystals (Fig. 5a), PEG 4000 was in a compact mass, and ES 100 was in spherical shape (Fig. 5c), respectively. The prismatic crystals of the free R1, the spherical ES 100 and the massive PEG 4000 all could be seen in the physical mixture of R1, PEG 4000 and ES 100 (Fig. 5b). However, the R1-SD solid dispersion presented as a homogeneous, plate-like structure (Fig. 5d), and it was quite different from free R1 and the adjuvants. These results directly proved that the complete formation of R1-SD.

3.3.2. DSC analysis

DSC is a technique for measuring the temperature difference between a substance and a reference substance as a function of temperature, under the control of a temperature programme. If drug crystals are present in the solid dispersion, a heat absorption peak will appear; the more drug crystals there are, the larger the area of the heat absorption peak will be [35–37].

As shown in Fig. 6, free R1 had obvious characteristic of heat absorption peak at 118.7 °C (Fig. 6a), but there was no significant characteristic heat absorption peak in the physical mixture of PEG 4000 and ES 100 (Fig. 6c). The characteristic heat absorption peak of R1 disappeared in R1-SD (Fig. 6d), but existed in the physical mixture of R1, PEG 4000 and ES 100 (Fig. 6b), indicating that R1 was dispersed in an amorphous state in the carrier.

3.3.3. PXRD analysis

PXRD is widely used in the qualitative analysis of crystalline materials. Each crystalline substance has its own specific structure, and its powder diffraction pattern has its own characteristics. After the drug forms an amorphous solid dispersion, its characteristic crystal diffraction peak will disappear [35–37].

There was an obvious characteristic diffraction peak in free R1 (Fig. 7a), while no crystal diffraction peak was demonstrated in the physical mixture of PEG 4000 and ES 100 (Fig. 7c). Besides, the characteristic diffraction peak of the drug still existed in the physical mixture of R1, PEG 4000 and ES 100 (Fig. 7b). For R1-SD, the characteristic diffraction peak disappeared completely, indicating that R1 existed in amorphous form in R1-SD (Fig. 7d).

3.4. In vitro release of R1 and R1-SD

The *in vitro* release of R1 and R1-SD in human physiological pH changing environments was studied. Among them, R1 capsules and R1-SD capsules were released in gastric juice environment (hydrochloric acid solution at pH 1.2) for 2 h, small intestine environment (PBS at pH 6.8) for 4 h, and then transferred to colon environment (PBS at pH 7.8) for release. The experimental results are shown in Fig. 8. The cumulative release rate of R1 capsules at pH 1.2 for 2 h is about 40%, and the release rate exceeds 70% in PBS at pH 6.8 for 4 h, The release rate exceeds 80% in PBS with a pH value of 7.4 for 2 h. However, R1-SD capsules did not release at pH 1.2, with a release rate of less than 30% at pH 6.8 and over 90% at pH 7.6. The cumulative release rate of R1-SD meets the requirements of the Chinese Pharmacopoeia (2020 edition) for colon preparations. The significant release of R1 in the colon may be due to the pH sensitivity of the main supporting material ES 100, which can only dissolve under conditions with pH values above 7. Therefore, R1-SD can effectively prevent R1 from being destroyed under acidic conditions.

Three common drug release mathematical models were used to study the linear fitting curve of R1-SD at pH 7.6 as shown in Table 1.

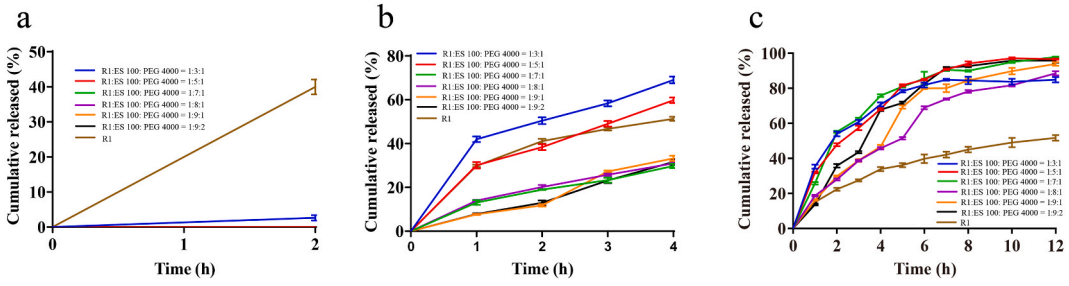

Fig. 4. *In vitro* cumulative releasing profiles of formulations with different ratio of ES 100 to PEG 4000. (a: pH 1.2. b pH 6.8. c pH 7.6).

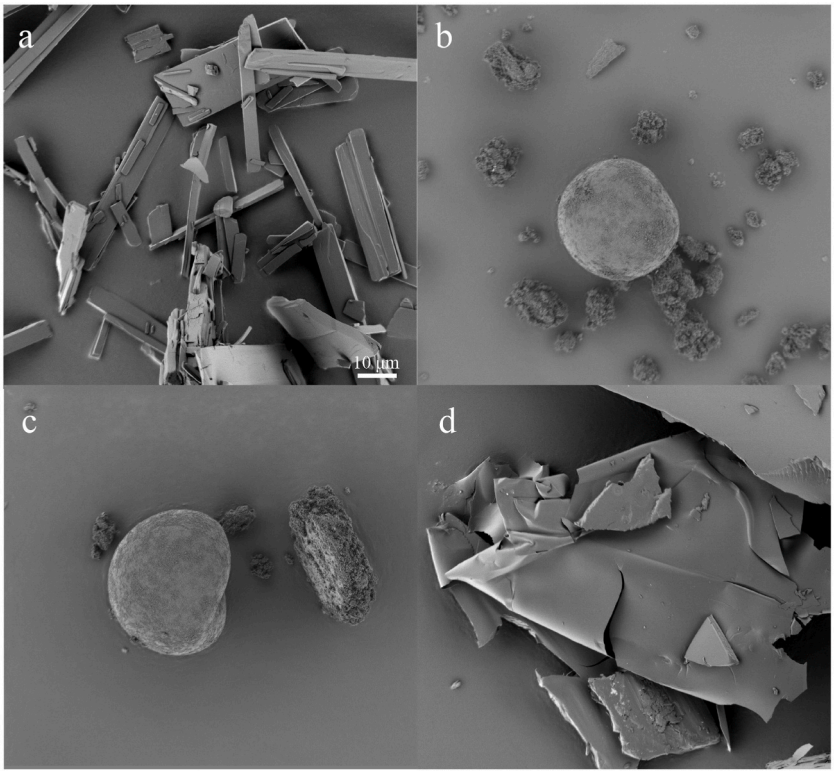

Fig. 5. SME photographs. (a: R1. b: Physical mixture of R1, PEG 4000 and ES 100. c: Physical mixture of PEG 4000 and ES 100. d: R1-SD.)

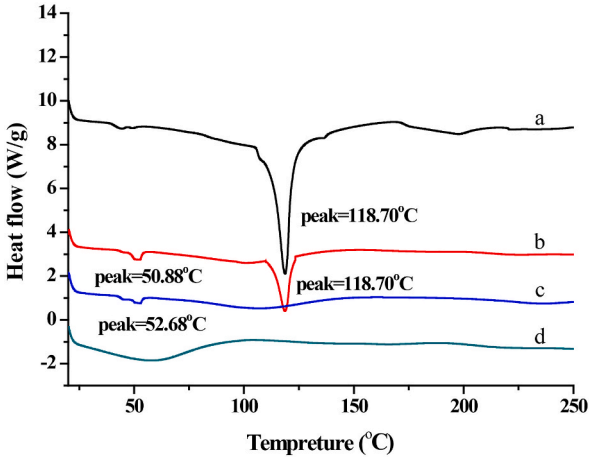

Fig. 6. DSC thermograms. (a: R1. b: Physical mixture of R1, PEG 4000 and ES 100. c: Physical mixture of PEG 4000 and ES 100. d: R1-SD.)

As can be seen from Table 1, the optimal linear fitting for R1-SD release was Higuchi release model with R^2 was the highest close to 1. It means that the drug in R1-SD is mainly released in the form of diffusion [38].

3.5. In vitro intestinal absorption of R1 and R1-SD

Comparing with the cumulative ileum absorption of R1, a significant increase was observed in R1-SD group after 45 min ($p < 0.05$, Fig. 9). The increase of absorption was not obvious between 0 and 45 min might be related to the sustained release skeleton of ES 100 which a certain time for swelling to release was needed.

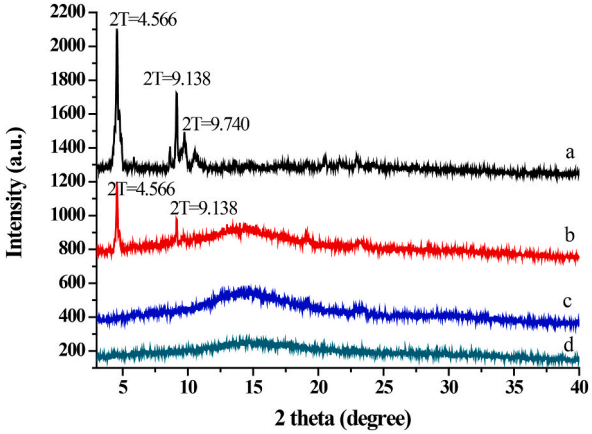

Fig. 7. PXRD patterns. (a: R1. b: Physical mixture of R1, PEG 4000 and ES 100. c: Physical mixture of PEG 4000 and ES 100. d: R1-SD.)

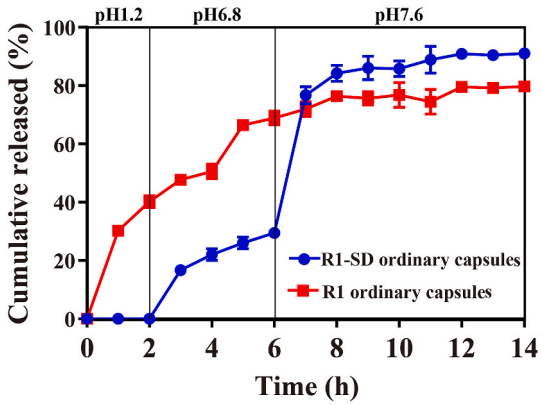

Fig. 8. *In vitro* cumulative releasing profiles of R1 and R1-SD ($n = 3$).

Table 1
Fitting of release kinetic equations.

Release models	Fitting equation	R^2
Zero-order (a)	$Q = 0.0178\ t + 0.4934$	0.8173
First-order (b)	$\ln (1\text{-}Q) = -0.0404\ t - 0.6750$	0.8475
Higuchi (c)	$Q = 0.0725\ t^{1/2} + 0.4256$	0.8945

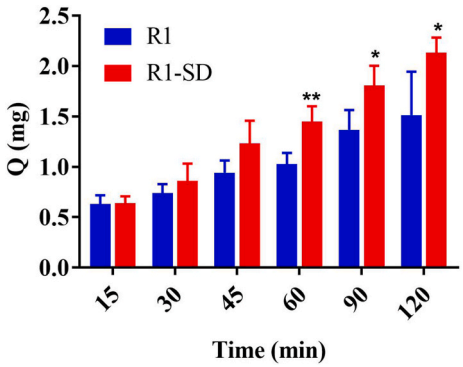

Fig. 9. Cumulative intestinal absorption of R1 and R1-SD ($n = 5$).

3.6. Protective effects on DSS colitis mice of R1 and R1-SD

DSS-induced colitis model has been widely used to elucidate the pathogenesis of UC [39]. Animals are orally administrated with 4% DSS water solution for 6–10 days, and the inflammatory reaction usually affects the mucosal lining of the intestinal wall, and the characteristics of the disease are similar to those of human [40]. In this study, R1 treatment could alleviated the inflammation symptoms such as bloody diarrhea, body colon shortening, weight loss, and histologic damage [5].

To evaluate whether the effect of R1-SD on DSS colitis model mice was correspond to or better than that of R1, efficacy based on some indexes of colitis was examined.

3.6.1. Changes in colonic morphology and length of UC mice

The results are shown in Fig. 10a and b. After the mice were sacrificed, the appearance of the colon in the vehicle group were normal, without erosion, congestion and ulcer, and there were feces formed in the colon. While, in the DSS model group, the colon was shortened obviously with severe edema, hemorrhage, and hyperemia occurred in the colon tissue, as well as severe ulcerations in the mucosa were observed. In addition, no feces was formed in the colon.

In the R1 group and R1-SD group, the states of hyperemia and edema were significantly alleviated accompany with the area reduction of ulcer necrosis and the elongating colon. At the same time, formed feces could be observed in the colon of mice in the R1-SD group. Significant differences were found in both R1 group and R1-SD group compared to the model group ($p < 0.05$, $p < 0.01$).

3.6.2. Changes in blood stool of UC mice

During the whole modeling process, the blood stool of mice were recorded every day and scored according to the classic histological injury scoring criteria of Cooper et al. [41]. After DSS water was given for 5 days (the 7th day in Fig. 10c), diarrhea began to appear in the model group, and there was a remarkable difference between the model group and the vehicle group ($p < 0.05$). The degree of diarrhea and bloody stool in the R1-SD group was alleviated more obviously than that in the R1 group. The R1-SD group significantly inhibited the blood stool of UC mice from day 8 ($p < 0.01$), while the R1 group also significantly inhibited the blood stool of mice from day 10 ($p < 0.01$) (Fig. 10c).

3.6.3. Changes in body weight of UC mice

During the whole experiment, it was found that the mice in the vehicle group had sensitive reactions with smooth and shiny fur, and gradually increased their weight. In contrast, after drinking DSS water for 2–4 days, depression and reduced food intake occurred in DSS model group, although there was no obvious change in fecal status and body weight. After drinking DSS water for 5–9 days, the rats in the model group showed hematochezia, fur lackluster, aggravation of depression, cluster, reduction of diet and water, and their body weights were significantly lower than those in the vehicle group ($p < 0.01$).

In the early stage of DSS inducing, there was a tendency to inhibit body weight loss both in the R1 group and R1-SD group, but no obvious difference was found between the drug treatment group and the DSS model group. The R1-SD group showed a significant inhibition of weight loss on the 8th day after a 6-day treatment ($p < 0.001$), on the other hand, the R1 group was able to significantly inhibit body weight loss in UC mice on day 9 ($p < 0.05$) (Fig. 10d).

3.6.4. Changes in spleen weight of UC mice

The spleen weight of the DSS induced model mice increased significantly comparing with the vehicle group ($p < 0.001$). Both the R1 group and R1-SD group could significantly inhibit the increase of spleen weights of mice ($p < 0.001$) which were close to that of the vehicle group. But there was no statistic difference between the R1 group and R1-SD group (Fig. 10e).

3.6.5. Histopathological changes and microscopic scores

The histopathological changes in each group were presented in Fig. 11A. The morphology of colon in the vehicle group was normal under microscope (Fig. 11Aa). On the other hand, colon epithelial cells in DSS model group arranged disorderly with large areas of necrosis and exfoliation. Hyperemia and thickening of intestinal wall, significant reduction of goblet cells, disorganized glandular structure, and inflammatory cell infiltration in the submucosa were also observed in the DSS model group (Fig. 11Ab). The R1 group (Fig. 11Ac) and R1-SD group (Fig. 11Ad) showed moderate edema of submucosa and mild inflammatory changes of mucosa and submucosa. The structure of glands in the R1-SD group was similar to that of the vehicle group, but the glandular structure of R1 group was still slightly disordered.

The microscopic scores of each group are presented in Fig. 11B. The loss of superficial epithelium, infiltrations of monocyte and neutrophils, hemorrhage, and edema were discovered in the DSS group. Moreover, the depth and width of ulcer lesion in the vehicle group were significantly different from those in the DSS model group ($p < 0.001$). Those results indicated that the colitis model was built successfully. Besides, the above ulcerative changes in the DSS model group were also significantly different from those in the R1 group ($p < 0.05$) and the R1-SD group ($p < 0.001$).

These results indicated that both R1 and R1-SD treatment could reduce the extent of colon hyperemia, edema and shortening, alleviate the degrees of diarrhea and bloody stool, as well as inhibit the body weight loss and spleen weight increase. The same effects could also be seen in the histopathological changes, such as reducing the areas of necrosis and exfoliation, improving the structure of glands, as well as alleviating the degree of the adhesiveness and infiltration of inflammatory cell in the submucosa. In addition, the protective effect of R1-SD on DSS colitis mice was significantly better than that of R1, which might be related to the better stability in acidic gastric environment and more absorption in colon of R1-SD.

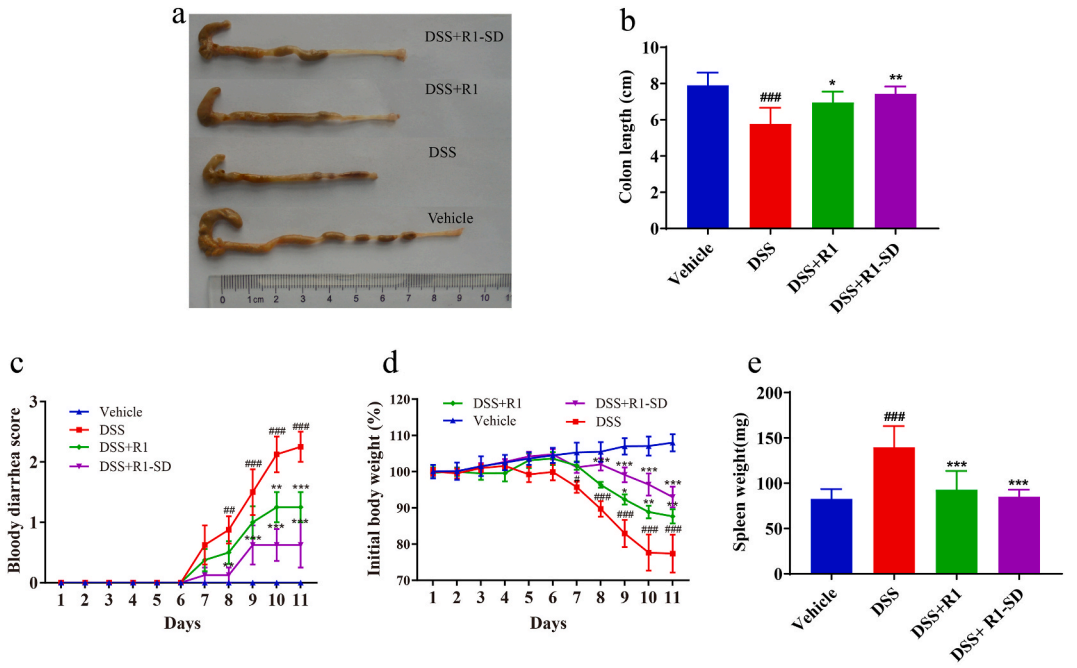

Fig. 10. R1 and R1-SD attenuated DSS-induced colitis in mice. (a: Macroscopic observation of colon shortening. b: Assessment of colon shortening. c: The occurrence of bloody diarrhea, the data are plotted as a percentage of the total mice that had bloody diarrhea at different time points of DSS treatment. d: Changes in body weight following DSS induction of colitis, the data are plotted as a percentage of the original body weight. e: Spleen weight of each group. $n = 10$. $^{\#}p < 0.05$, $^{\#\#}p < 0.01$, and $^{\#\#\#}p < 0.001$ *vs.* vehicle group; $^{*}p < 0.05$, $^{**}p < 0.01$, and $^{***}p < 0.001$ *vs.* DSS model group.)

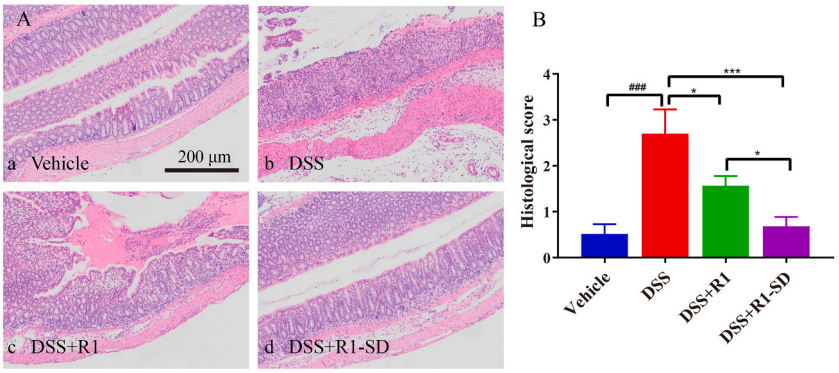

Fig. 11. Pathological analysis results of colon tissues. (A: Representative H & E-stained colon sections, magnification 200 × . B: Histology scoring for H & E-stained colon sections. $n = 10$. $^{\#\#\#}p < 0.001$ *vs.* vehicle group; $^{*}p < 0.05$, $^{***}p < 0.001$ *vs.* DSS model group.)

4. Conclusion

In this study, a pH-dependent colon-targeted drug delivery system of R1 was designed to maximize the release of R1 in the colon and improve its oral absorbability. R1-SD, a pH-dependent solid dispersion preparation, was fabricated by solvent evaporation method, in which R1 was existed in an amorphous state in ES 100 and PEG 4000. R1-SD confirms to the requirements for colon soluble preparations, that is pH 1.2 insolubility, pH 6.8 low solubility and pH 7.6 high solubility. The absorption rate and cumulative release of R1-SD were higher than those of R1 according to the *in vitro* colon absorption. Moreover, R1-SD showed much better protective effect on DSS induced colitis mice than that of R1, which could compensate the shortcomings of R1 including poor oral absorption and easy decomposition in the gastric area.

Those above research has laid the foundation for the further development and application of R1. The fabrication process of R1-SD is simple, with high reproducibility, controllable quality, and good stability, demonstrating good anti-colitis effects. It is expected to be developed as a new formulation for treating colitis.

Author contribution statement

Hongyun Tie, Yaru Wang: Performed the experiments; Analyzed and interpreted the data; Wrote the paper.
Yunxia Shang: Performed the experiments.
Manlin Li: Analyzed and interpreted the data; Wrote the paper.
Xiaohui Wei: Conceived and designed the experiments; Contributed reagents, materials, analysis tools or data; Wrote the paper.
Zhengtao Wang: Conceived and designed the experiments.

Data availability statement

Data will be made available on request.

Declaration of competing interest

The authors declare that they have no known competing financial interests or personal relationships that could have appeared to influence the work reported in this paper.

Acknowledgements

This work was supported by the Shanghai Municipal Education Commission [grant number A1-GY20-306-02-07].

References

[1] W. Wang, L. Huang, Y. Hu, E.R. Thomas, X. Li, Neuroprotective effects of notoginsenoside R1 by upregulating Trx-1 on acrylamide-induced neurotoxicity in PC12, Hum. Exp. Toxicol. 39 (6) (2020) 797–807, https://doi.org/10.1177/0960327120901586.
[2] D.L. Qian, X.K. Shao, Y. Li, X. Sun, Notoginsenoside R1 protects WI-38 cells against lipopolysaccharide-triggered injury via adjusting the miR-181a/TLR4 axis, J. Cell. Biochem. 120 (12) (2019) 19764–19774, https://doi.org/10.1002/jcb.29282.
[3] Y. Yu, G. Sun, Y. Luo, M. Wang, R. Chen, J. Zhang, Q. Ai, N. Xing, X. Sun, Cardioprotective effects of Notoginsenoside R1 against ischemia/reperfusion injuries by regulating oxidative stress- and endoplasmic reticulum stress- related signaling pathways, Sci. Rep. 6 (2016), 21730, https://doi.org/10.1038/srep21730.
[4] C.Z. Wang, J.T. Xie, A. Fishbein, H.H. Aung, H. He, S.R. Mehendale, T.C. He, W. Du, C.S. Yuan, Antiproliferative effects of different plant parts of Panax notoginseng on SW480 human colorectal cancer cells, Phytother Res. 23 (1) (2009) 6–13, https://doi.org/10.1002/ptr.2383.
[5] J. Zhang, L. Ding, B. Wang, G. Ren, A. Sun, C. Deng, X. Wei, S. Mani, Z. Wang, W. Dou, Notoginsenoside R1 attenuates experimental inflammatory bowel disease via pregnane X receptor activation, J. Pharmacol. Exp. Ther. 352 (2) (2015) 315–324, https://doi.org/10.1124/jpet.114.218750.
[6] Q. Fan, Y. Zhang, X. Hou, Z. Li, K. Zhang, Q. Shao, N. Feng, Improved oral bioavailability of notoginsenoside R1 with sodium glycocholate-mediated liposomes: preparation by supercritical fluid technology and evaluation in vitro and in vivo, Int. J. Pharm. 552 (1–2) (2018) 360–370, https://doi.org/10.1016/j.ijpharm.2018.10.005.
[7] F. Liang, J.X. Hua, Absorption profiles of sanchinoside R1 and ginsenoside Rg1 in the rat intestine, Eur. J. Drug Metab. Pharmacokinet. 30 (4) (2005) 261–268, https://doi.org/10.1007/bf03190630.
[8] H. Hasegawa, J.H. Sung, S. Matsumiya, M. Uchiyama, Main ginseng saponin metabolites formed by intestinal bacteria, Planta Med. 62 (5) (1996) 453–457, https://doi.org/10.1055/s-2006-957938.
[9] X. Li, J. Sun, G. Wang, H. Hao, Y. Liang, Y. Zheng, B. Yan, L. Sheng, Simultaneous determination of panax notoginsenoside R1, ginsenoside Rg1, Rd, Re and Rb1 in rat plasma by HPLC/ESI/MS: platform for the pharmacokinetic evaluation of total panax notoginsenoside, a typical kind of multiple constituent traditional Chinese medicine, Biomed. Chromatogr. 21 (7) (2007).
[10] X. Li, G. Wang, J. Sun, H. Hao, Y. Xiong, B. Yan, Y. Zheng, L. Sheng, Pharmacokinetic and absolute bioavailability study of total panax notoginsenoside, a typical multiple constituent traditional Chinese medicine (TCM) in rats, Biol. Pharm. Bull. 30 (5) (2007) 847–851, https://doi.org/10.1248/bpb.30.847.
[11] H.Y. Kim, J.H. Cheon, S.H. Lee, J.Y. Min, S.Y. Back, J.G. Song, D.H. Kim, S.J. Lim, H.K. Han, Ternary nanocomposite carriers based on organic clay-lipid vesicles as an effective colon-targeted drug delivery system: preparation and in vitro/in vivo characterization, J. Nanobiotechnology 18 (1) (2020) 17–32, https://doi.org/10.1186/s12951-020-0579-7.
[12] Y.S.R. Krishnaiah, P. Veer Raju, B. Dinesh Kumar, V. Satyanarayana, R.S. Karthikeyan, P. Bhaskar, Pharmacokinetic evaluation of guar gum-based colon-targeted drug delivery systems of mebendazole in healthy volunteers, J. Control. Release 88 (1) (2003) 95–103, https://doi.org/10.1016/s0168-3659(02)00483-2.
[13] D. Liu, H. Yan, Y. Kong, Y. You, Y. Li, L. Wang, Y. Tong, J. Wang, Preparation of colon-targeted acetylharpagide tablets and its release properties in vivo and in vitro, Front. Pharmacol. 9 (2018) 832, https://doi.org/10.3389/fphar.2018.00832.
[14] M. Naeem, U.A. Awan, F. Subhan, J. Cao, S.P. Hlaing, J. Lee, E. Im, Y. Jung, J.W. Yoo, Advances in colon-targeted nano-drug delivery systems: challenges and solutions, Arch Pharm. Res. (Seoul) 43 (1) (2020) 153–169, https://doi.org/10.1007/s12272-020-01219-0.
[15] M.M. Patel, A.F. Amin, Design and optimization of colon-targeted system of theophylline for chronotherapy of nocturnal asthma, J. Pharm. Sci. 100 (5) (2011) 1760–1772, https://doi.org/10.1002/jps.22406.
[16] L. Zhang, Y. Sang, J. Feng, Z. Li, A. Zhao, Polysaccharide-based micro/nanocarriers for oral colon-targeted drug delivery, J. Drug Target. 24 (7) (2016) 579–589, https://doi.org/10.3109/1061186X.2015.1128941.
[17] H. Chauhan, C. Hui-Gu, E. Atef, Correlating the behavior of polymers in solution as precipitation inhibitor to its amorphous stabilization ability in solid dispersions, J. Pharm. Sci. 102 (6) (2013) 1924–1935, https://doi.org/10.1002/jps.23539.
[18] D.D. Hu, L. Liu, W.J. Chen, S.N. Li, Y.P. Zhao, A novel preparation method for 5-aminosalicylic acid loaded Eudragit S100 nanoparticles, Int. J. Mol. Sci. 13 (5) (2012) 6454–6468, https://doi.org/10.3390/ijms13056454.
[19] D.S. Jones, Y. Tian, S. Li, T. Yu, O.A. Abu-Diak, G.P. Andrews, The use of binary polymeric networks in stabilizing polyethylene oxide solid dispersions, J. Pharm. Sci. 105 (10) (2016) 3064–3072, https://doi.org/10.1016/j.xphs.2016.06.004.
[20] J.H. Park, H.K. Choi, Enhancement of solubility and dissolution of cilostazol by solid dispersion technique, Arch Pharm. Res. (Seoul) 38 (7) (2015) 1336–1344, https://doi.org/10.1007/s12272-014-0547-6.
[21] Q. Xu, N. Zhang, W. Qin, J. Liu, Z. Jia, H. Liu, Preparation, in vitro and in vivo evaluation of budesonide loaded core/shell nanofibers as oral colonic drug delivery system, J. Nanosci. Nanotechnol. 13 (1) (2013) 149–156, https://doi.org/10.1166/jnn.2013.6920.
[22] M. Maghsoodi, F. Sadeghpoor, Preparation and evaluation of solid dispersions of piroxicam and Eudragit S100 by spherical crystallization technique, Drug Dev. Ind. Pharm. 36 (8) (2010) 917–925, https://doi.org/10.3109/03639040903585127.

[23] C. Liu, K.G. Desai, Characteristics of rofecoxib-polyethylene glycol 4000 solid dispersions and tablets based on solid dispersions, Pharm. Dev. Technol. 10 (4) (2005) 467–477, https://doi.org/10.1080/10837450500299701.
[24] L.X. Liu, X.C. Wang, Improved dissolution of oleanolic acid with ternary solid dispersions, AAPS PharmSciTech 8 (4) (2007) 267–271, https://doi.org/10.1208/pt0804113.
[25] D.M. Patel, S.P. Patel, C.N. Patel, Formulation and evaluation of fast dissolving tablet containing domperidone ternary solid dispersion, Int. J. Pharm. Investig. 4 (4) (2014) 174–182, https://doi.org/10.4103/2230-973x.143116.
[26] J. Wendelboe, M.M. Knopp, F. Khan, N. Chourak, T. Rades, R. Holm, Importance of in vitro dissolution conditions for the in vivo predictability of an amorphous solid dispersion containing a pH-sensitive carrier, Int. J. Pharm. 531 (1) (2017) 324–331, https://doi.org/10.1016/j.ijpharm.2017.08.078.
[27] L.R. Brun, M.L. Brance, M. Lombarte, M. Lupo, V.E. Di Loreto, A. Rigalli, Regulation of intestinal calcium absorption by luminal calcium content: role of intestinal alkaline phosphatase, Mol. Nutr. Food Res. 58 (7) (2014) 1546–1551, https://doi.org/10.1002/mnfr.201300686.
[28] A. Das, A.K. Nayak, B. Mohanty, S. Panda, Solubility and dissolution enhancement of etoricoxib by solid dispersion technique using sugar carriers, ISRN Pharm 2011 (2011), 819765, https://doi.org/10.5402/2011/819765.
[29] C. Inigo, N. Patel, G.L. Kellett, A. Barber, M.P. Lostao, Luminal leptin inhibits intestinal sugar absorption in vivo, Acta Physiol. 190 (4) (2007) 303–310, https://doi.org/10.1111/j.1748-1716.2007.01707.x.
[30] S. Okonogi, S. Puttipipatkhachorn, Dissolution improvement of high drug-loaded solid dispersion, AAPS PharmSciTech 7 (2) (2006) E52, https://doi.org/10.1208/pt070252.
[31] C.D. Tran, J.M. Ball, S. Sundar, P. Coyle, G.S. Howarth, The role of zinc and metallothionein in the dextran sulfate sodium-induced colitis mouse model, Dig. Dis. Sci. 52 (9) (2007) 2113–2121, https://doi.org/10.1007/s10620-007-9765-9.
[32] W. Dou, J. Zhang, E. Zhang, A. Sun, L. Ding, G. Chou, Z. Wang, S. Mani, Chrysin ameliorates chemically induced colitis in the mouse through modulation of a PXR/NF-κB signaling pathway, J. Pharmacol. Exp. Ther. 345 (3) (2013) 473–482, https://doi.org/10.1124/jpet.112.201863.
[33] M.S. Geier, R.N. Butler, P.M. Giffard, G.S. Howarth, Lactobacillus fermentum BR11, a potential new probiotic, alleviates symptoms of colitis induced by dextran sulfate sodium (DSS) in rats, Int. J. Food Microbiol. 114 (3) (2007) 267–274, https://doi.org/10.1016/j.ijfoodmicro.2006.09.018.
[34] G. Ren, A. Sun, C. Deng, J. Zhang, X. Wu, X. Wei, S. Mani, W. Dou, Z. Wang, The anti-inflammatory effect and potential mechanism of cardamonin in DSS-induced colitis, Am. J. Physiol. Gastrointest. Liver Physiol. 309 (7) (2015) G517–G527, https://doi.org/10.1152/ajpgi.00133.2015.
[35] D.R. Telange, N.M. Bhaktani, A.T. Hemke, A.M. Pethe, S.S. Agrawal, N.R. Rarokar, S.P. Jain, development and characterization of pentaerythritol-EudragitRS100 Co-processed excipients as solid dispersion carriers for enhanced aqueous solubility, dissolution, and permeation of atorvastatin.[J], ACS Omega 8 (2023) 25195–25208, https://doi.org/10.1021/acsomega.3c02280.
[36] A. Budiman, N.V. Nurani, E. Laelasari, M. Muchtaridi, S. Sriwidodo, D.L. Aulifa, Effect of Drug-Polymer Interaction in Amorphous Solid Dispersion on the Physical Stability and Dissolution of Drugs: the Case of Alpha-Mangostin, Polymers, Basel, 2023, https://doi.org/10.3390/polym15143034.
[37] D. Mohapatra, D.N. Kumar, S. Shreya, V. Pandey, P.K. Dubey, A.K. Agrawal, A.N. Sahu, Quality by Design-Based Development and Optimization of Fourth-Generation Ternary Solid Dispersion of Standardized Piper Longum Extract for Melanoma Therapy, Drug Deliv Transl Res, 2023. https://doi:10.1007/s13346-023-01375-y.
[38] P.L. Ritger, N.A. Peppas, A simple equation for description of solute release I. Fickian and non-fickian release from non-swellable devices in the form of slabs, spheres, cylinders or discs, J Control Release 5 (1) (1987) 23–36. https://doi:10.1016/0168-3659(87)90034-4.
[39] F. Zhou, N. Wang, L. Yang, L.C. Zhang, L.J. Meng, Y.C. Xia, Saikosaponin A protects against dextran sulfate sodium-induced colitis in mice, Int. Immunopharmacol. 72 (2019) 454–458, https://doi.org/10.1016/j.intimp.2019.04.024.
[40] Y.W. Wu, B. Wu, Z.W. Zhang, H.M. Lu, C. Fan, Q. Qi, Y.Z. Gao, H. Li, C.L. Feng, J.P. Zuo, W. Tang, Heme protects intestinal mucosal barrier in DSS-induced colitis through regulating macrophage polarization in both HO-1-dependent and HO-1-independent way, FASEB J 34 (6) (2020) 8028–8043, https://doi.org/10.1096/fj.202000313RR.
[41] H.S. Cooper, S.N. Murthy, R.S. Shah, D.J. Sedergran, Clinicopathologic study of dextran sulfate sodium experimental murine colitis, Lab. Invest. 69 (2) (1993) 238–249.